ISSN 1392-1207. MECHANIKA. Vol. 29, No. 5, 2023: 395–404

Model Updating Based on Bayesian Theory and Improved Objective Function

Ming ZHAI*, Yikui XIE**
**Zhengzhou University, No.100 Science Avenue, Zhengzhou City, Henan Province P. R. China,*
E-mail: 1355975289@qq.com
***Zhengzhou University, No.100 Science Avenue, Zhengzhou City, Henan Province P.R.China,*
E-mail: xieyikui1998@163.com
https://doi.org/10.5755/j02.mech.33244

1. Introduction

The finite element (FE) model method is widely used in the field of structural engineering and is an important part of computer-aided design. The application of the FE method for analysis can reduce the time and economic cost, and also provide a theoretical guarantee for the feasibility of the design scheme. However, due to the idealized treatments of the structure in the process of the FE modelling, there is a certain deviation between the FE model and the actual structure. If the deviation exceeds the allowable range, the credibility of the constructed FE model will be questioned and the analytical results will lose its value. The FE model updating theory is developed consequently to calibrate the FE model. The updated FE model has practical significance for structural health monitoring [1] and condition evaluation [2].

The basic idea of model updating methods is to make the FE model produce a theoretical response that is as consistent as possible with the test data by adjusting the selected uncertain structural parameters [3-4]. The updated parameters are not limited to the material properties of each element, but can also include the geometric parameters of the structure, boundary conditions, etc. Model updating methods are divided into direct methods and iterative methods. The focus of the direct methods is to update the matrix of the dynamic system [5] so that the predicted numerical results match the experimental results. However, the updated theoretical model lost its original physical meaning. On the other hand, the iterative methods update structural physical parameters and have been widely used. Model updating based on the iterative method can be regarded as an optimization problem [6], and its steps include the selection of updated parameters, the construction of objective functions, and the selection of optimization algorithms.

In the iterative methods, the physical parameters of the model are successively updated by the sensitivity methods. The effectiveness of the sensitivity-based FE model updating methods has been verified in various applications. For example, the model updating of the three-beam composite structure [7], the cantilever bar of a boring bar [8], the FE model of Shanghai Tower [9], the three-dimensional nonlinear structure [10], etc. However, the sensitivity-based FE model updating methods usually need to establish sensitivity matrixes to update parameters, which is not suitable for large structures due to the high cost of computation. To improve computational efficiency and reduce the cost of computation, meta-model methods have been developed. The meta-model methods obtain relatively simple proxy models by fitting the sample data of the FE model, such as the optimal polynomial response surface model [11], the Polynomial-chaotic Kriging (PCK) [12], the vectorial surrogate modeling (VSM) approach [13], the Gaussian process (GP) regression [14], the adaptive metamodel [15], etc. However, the accuracy of meta-model methods is relatively low and highly related to the determination of sample space. Improper sample selection will lead to inadequate generalization ability of meta-model and unreliable updating results. As an optimization problem, the efficiency and results of model updating also depend on the ability of the optimization algorithm to deal with complex FE models. Many optimization algorithms have been developed and improved, such as the sequential quadratic programming (SQP) algorithm [16], the improved particle swarm optimization (IPSO) algorithm [17], the evolutionary algorithm [18], the derivative-free optimization algorithm [19], the direct updating algorithm [20], the improved meta-heuristic algorithm [21], etc. In addition, the FE model updating methods based on statistics and probability have been gradually applied in different applications. For example, the failure probability is used to predict the remaining service life [22], the Bayesian data fusion method is applied to find the exact location of damage [23], the semi-supervised learning method of transferred Bayesian learning (TBL) is used to the building structure [24], the Markov chain Monte Carlo parallel technique is applied to an office building [25], etc. However, the FE model updating methods based on statistics and probability need to solve the complex integration and determine the distribution of all variables, so the computation cost is high.

The focus of this paper is to improve the existing model updating method to improve its computational efficiency and accuracy. Selecting proper parameters is of great importance to the model updating process. Updating too many parameters not only increases the cost of computation but also causes ill-posed problems which will lead to the failure of the updating process. To improve the efficiency of model updating, a natural frequency damage index (NFDI) based on the Bayesian theory is introduced to select the updated parameters. The NFDI is easy to establish and can quickly identify the damaged location of the structure and the updated parameters can be determined according to the identified damage location consequently. On the other hand, an objective function of strain assurance criterion (SAC) type is proposed to improve the accuracy of model updating. The weight coefficients determined based on the sensitivity analysis are employed for the proposed objective function.

The accuracy of the proposed objective function is compared with that of the ordinary least square method.

The rest of this paper is described as follows. Section 2 introduces the model updating method and describes the key steps in detail. Section 3 analyzes a beam model and the efficiency of the improved method for selecting updated parameters is verified. Section 4 verifies the updated accuracy of the improved objective function with a pressure container model. The conclusions are drawn in section 5.

2. The model updating method

This paper employed iterative method to update FE model, and the updating process is shown in Fig. 1. The steps are given as follows:

1. Establish the FE model according to the actual structure.
2. Select the appropriate updated parameters and set their range.
3. Construct the objective function.
4. Select the appropriate optimization algorithm.
5. Perform convergence judgment and output optimization results.

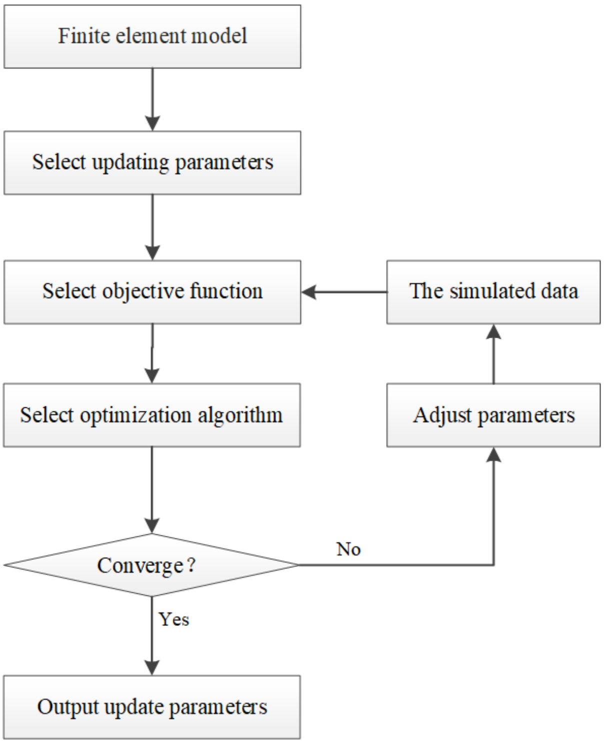

Fig. 1 The model updating method

2.1. Selecting updated parameters based on NFDI identification

The selection of updated parameters largely determines the result of the model updating. Updating too many parameters will not only increase the cost of computation but also lead to non-convergence errors and other problems. Different from the empirical method or sensitivity method [26], the NFDI is configured based on Bayesian theory to select the updated parameters to improve the efficiency of model updating.

The natural frequency of a structure is related to its stiffness and mass distribution. Cracks will lead to the reduction of structural stiffness and natural frequency. The characteristic curves of natural frequency variation and damage location are obtained based on Bayesian theory. Then, according to the measured frequency data, the NFDI is constructed to identify the damage location [27]. The process of establishing the damage position function and the NFDI is as follows:

1. Define the characteristic curve of natural frequency variation and damage location. Firstly, the natural frequency values of undamaged and damaged model are obtained by simulation. Then the natural relative frequency change (RNFC) $\Delta\omega_j$ is calculated as follows:

$$\Delta\omega_j\left(\zeta_i\right)=\frac{\omega_j-\omega_j^d\left(\zeta_i\right)}{\omega_j}, \tag{1}$$

where: $\Delta\omega_j$ represents the jth RNFC; ζ_i represents the damage location; ω_j represents the jth natural frequency of the undamaged model, and ω_j^d represents the jth natural frequency of the damaged model. By standardizing $\Delta\omega_j$ to the interval of [0, 1], the normalized RNFC $\Delta\overline{\omega_j}$ can be obtained as follows:

$$\Delta\overline{\omega_j}\left(\zeta_i\right)=\frac{\Delta\omega_j\left(\zeta_i\right)-min\left(\Delta\omega_j\left(\zeta_i\right)\right)}{max\left(\Delta\omega_j\left(\zeta_i\right)\right)-min\left(\Delta\omega_j\left(\zeta_i\right)\right)}, \tag{2}$$

where: $max\left(\Delta\omega_j\left(\zeta_i\right)\right)$ and $min\left(\Delta\omega_j\left(\zeta_i\right)\right)$ represent the maximum and minimum values of RNFC at all damage locations under jth order, respectively. The characteristic curve $g_j\left(\zeta\right)$ is defined as the RNFC curve:

$$g_j\left(\zeta\right)=\Delta\overline{\omega_j}\left(\zeta_i\right), \tag{3}$$

where: ζ represents all damage locations.

2. Calculate the measured RNFC after normalization. The natural frequency values of undamaged and damaged structure are obtained by test, and the jth measured RNFC $\Delta\omega_{mj}$ can be calculated as follows:

$$\Delta\omega_{mj}=\frac{\omega_{mj}-\omega_{mj}^d}{\omega_{mj}}, \tag{4}$$

where: ω_{mj} represents the jth measured natural frequency of the undamaged structure, and ω_{mj}^d represents the jth measured natural frequency of the damaged structure. By standardizing $\Delta\omega_{mj}$ to the interval of [0, 1], the measured RNFC after normalization can be obtained as follows:

$$\Delta\overline{\omega_{mj}}=\frac{\Delta\omega_{mj}-min\left(\Delta\omega_{mj}\right)}{max\left(\Delta\omega_{mj}\right)-min\left(\Delta\omega_{mj}\right)}, \tag{5}$$

where: $max\left(\Delta\omega_{mj}\right)$ and $min\left(\Delta\omega_{mj}\right)$ represent the maximum and minimum values of the measured RNFC under all orders respectively.

3. Define the jth damage position function (DPF):

$$DPF_j = 1 - \left| g_j(\zeta) - \Delta\overline{\omega_{mj}} \right|, \tag{6}$$

where: $g_j(\zeta)$ is the RNFC curve, which is selected according to the characteristics of the problem under study.

4. Data fusion of multi-order DPF function. As an effective data fusion method, Bayesian data fusion has been successfully applied in the field of structural damage diagnosis. Assuming that there are M information sources as $S_1, S_2, \cdots, S_M$, there are N events as $A_1, A_2, \cdots, A_N$ to be identified. The prior probability of A_i event is denoted as $P(A_i)$, and the conditional probability of event A_i is denoted as $P(S_1, S_2, \cdots, S_M | A_i)$. According to the Bayes formula, Bayesian fusion can be expressed as:

$$P(A_i | S_1, S_2, \cdots, S_M) = \frac{P(S_1, S_2, \cdots, S_M | A_i) P(A_i)}{\sum_{i=1}^{N} \left(P(S_1, S_2, \cdots, S_M | A_i) P(A_i) \right)}, \tag{7}$$

when the decisions from each information source are independent, Eq. (7) can be further denoted as:

$$P(A_i | S_1, S_2, \cdots, S_M) = \frac{\prod_{j=1}^{M} P(S_j | A_i) P(A_i)}{\sum_{i=1}^{N} \left(\prod_{j=1}^{M} P(S_j | A_i) P(A_i) \right)}. \tag{8}$$

In this study, the information source S_j was represented by the jth natural frequency, and the event A_i is represented by the occurrence of damage at ith element. The prior probability of A_i event is set as $P(A_i) = 1/N$. The conditional probability of the event A_i is:

$$P(S_j | A_i) = DPF_{i,j}, \tag{9}$$

where: $DPF_{i,j}$ is the value of DPF_j curve at the ith position. According to Eq. (8), the Bayesian fusion result is:

$$P(A_i | S_1, S_2, \cdots, S_M) = \frac{\prod_{j=1}^{M} DPF_{i,j}}{\sum_{i=1}^{N} \left(\prod_{j=1}^{M} DPF_{i,j} \right)}, \tag{10}$$

where: $P(A_i | S_1, S_2, \cdots, S_M)$ stands for Bayesian probability, denoted P_i.

5. Improvement of Bayesian probability. According to the symmetry characteristics of the model, the following improvements are made on Bayesian probability:

$$Q_i = \begin{cases} P_i, & \text{if not symmetrical} \\ \sqrt{P_i P_{N+1-i}}, & \text{if symmetrical} \end{cases}, \tag{11}$$

where: Q_i represents the improved Bayesian probability of the ith position, and P_{N+1-i} represents the Bayesian fusion result in a symmetric position with P_i.

6. Standardization:

$$Z_i = \frac{Q_i - \mu(Q)}{\sigma(Q)}. \tag{12}$$

where: $\mu(Q)$ represents the mean value of Q and $\sigma(Q)$ represents the standard deviation of Q.

7. Define the NFDI:

$$NFDI = \begin{cases} Z_i, & \text{if } Z_i \geq 0 \\ 0, & \text{if } Z_i < 0 \end{cases}. \tag{13}$$

The location of the maximum NFDI value has the highest possibility of damage. Therefore, the damaged location is determined by the maximum value of NFDI. After the damaged location is identified, the parameters of the location can be updated to improve the selection of updated parameters for the following model updating process.

2.2. The improved objective function

The objective function quantifies the difference between the actual structure and the FE model, which is usually defined as the residual difference between the experimental data of the actual structure and the computational features of the FE model. The model updating is to make the objective function reach the optimal value within a certain range. In the updating of the FE model, the objective function has a great influence on the updating result. In this paper, the strain residuals are used to configure the objective function. The optimization problem is:

$$min\left[F(x)\right]; \quad x \in S, \tag{14}$$

where: F is the objective function; x is the vector containing updated parameters, and S represents the feasible solution set in the decision space.

The most widely used objective function is configured based on generally OLS type [28], as shown in Eq. (15):

$$F_{OLS}(x^k) = \sum_{i=1}^{n} \left(\varepsilon_{m,i}(x) - \varepsilon_{a,i}(x^k) \right)^2, \tag{15}$$

where: x is the parameter that needs to be updated; k is the number of iterations; n is the number of measuring points; $\varepsilon_{m,i}(x)$ is the measured feature data of the sensor, and $\varepsilon_{a,i}(x^k)$ is the simulated feature data of the FE. In this paper, a new objective function type named SAC is configured as Eq. (16):

$$F_{SAC}(x^k) = 1 - \frac{\left(\sum_{i=1}^{n} \left(w_i^2 \cdot \varepsilon_{m,i}(x) \cdot \varepsilon_{a,i}(x^k) \right) \right)^2}{\sum_{i=1}^{n} \left(w_i \cdot \varepsilon_{m,i}(x) \right)^2 \cdot \sum_{i=1}^{n} \left(w_i \cdot \varepsilon_{a,i}(x^k) \right)^2}, \tag{16}$$

where: w_i is the weight of the ith measurement point.

The weight w_i is of great importance to the optimization process. It is determined as follows:

1. Calculate the sensitivity values. The structure is divided into several parts, and then each part is divided into d sub-parts. In this paper, the sensitivity refers to the derivative of the strain residual with respect to the updated parameter. For each part, the sensitivity value of each sub-part is calculated and d sensitivity values are obtained for each part.

2. Calculate the sensitivity coefficient of each part. The sensitivity coefficient is determined according to the sensitivity values of each part, and the statistical analysis results of the sensitivity values of each part show exponential regularity. Therefore, the sensitivity fitting function of the jth part is as follows:

$$F_j(y) = a_1 \cdot e^{-a_2 \cdot y}, \tag{17}$$

where: a_1 and a_2 are the coefficients obtained by fitting, and y is the number of the sub-parts from 1 to d. The above fitting function can be further changed to:

$$F_j(y) = b \cdot \frac{1}{\mu} e^{-\frac{y}{\mu}}, \tag{18}$$

where: b is the sensitivity coefficient; μ is the exponential coefficient; $\mu = 1/a_2$; $b = a_1 \cdot \mu$. By integrating the above formula, the result can be obtained as d tends to infinity:

$$P_j = \int F_j(y) = \int_0^{+\infty} b \cdot \frac{1}{\mu} e^{-\frac{y}{\mu}} dy = b. \tag{19}$$

Therefore, the sensitivity coefficient of this part can be represented by b.

3. Calculate the weight. After the sensitivity coefficients are calculated, the weight of the jth part calculation formula is as follows:

$$w_j = \frac{b_j}{\sum b_j}, \tag{20}$$

where: b_j represents the sensitivity fitting coefficient of the jth part. When the data x_i of the ith measurement point belongs to the jth part, the weight of the objective function is calculated as follows:

$$w_i = w_j. \tag{21}$$

3. Verification with beam model for NFDI identification

In this section, a beam model is analyzed and the accuracy of the NFDI identification based on Bayesian theory is verified. The updated parameters can be determined based on the identified result to improve the efficiency and accuracy of model updating.

3.1. Numerical example for NFDI identification

Ansys Workbench software was used to establish the numerical model, and the beam structure was shown in Fig. 2. Its length is 1000 mm, width is 30 mm, thickness is 3 mm, elastic modulus is 2.0×10^{11} Pa, Poisson's ratio is 0.3, and density is 7850 kg/m^3.

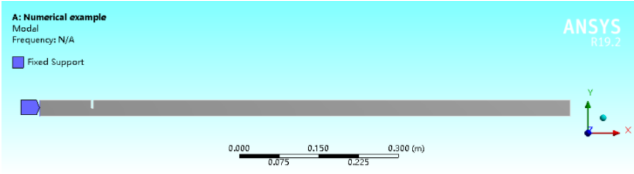

Fig. 2 The FE model of the beam

First, the normalized RNFC curves are calculated. The boundary conditions are cantilever beams. The simulated damage conditions were set with 15 mm deep and 4 mm wide cracks at 10 mm intervals. There were 100 damaged locations. After modal analysis of the model, 8 mode shape frequencies (1st, 2nd, 4th, 5th, 6th, 9th, 10th, 11th natural frequencies) were selected for analysis. After the natural frequency values of the undamaged and damaged beams are obtained through simulation, the normalized RNFC curves are calculated according to Eqs. (1) and (2). The result is shown in Fig. 3. It can be seen from the figure that the RNFC caused by the damage is a function of the damage position ζ_i.

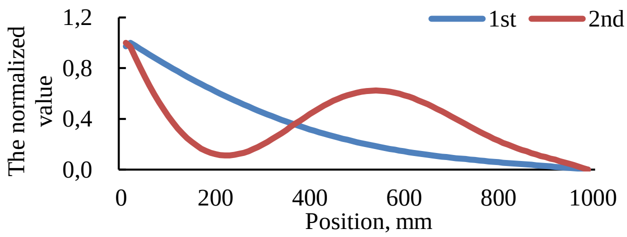

a

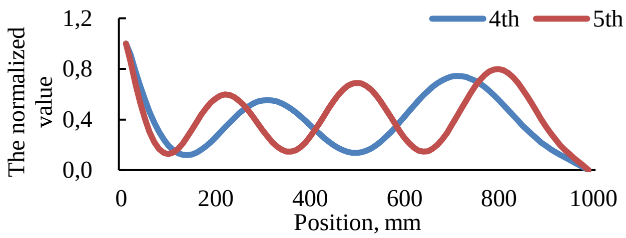

b

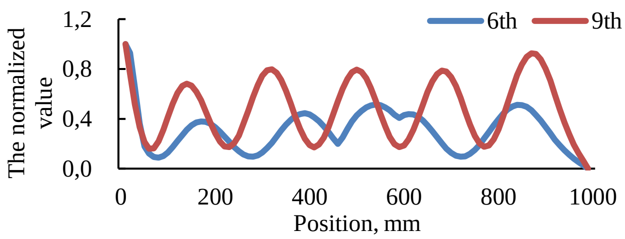

c

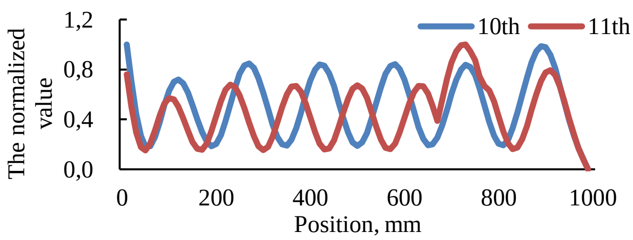

d

Fig. 3 The normalized curves of RNFC

Then, the measured RNFC values under different working conditions were calculated. The damage conditions are set to crack at 100 mm and 700 mm respectively. The natural frequencies of the undamaged and damaged beams are shown in Table 1. It can be seen that the natural frequencies decrease after damage occurs. The measured RNFC values after normalization of all orders are calculated according to Eq. (5), and the results are also listed in Table 1.

Finally, the NFDI values are calculated. The calculation results according to Eqs. (6) to (13) are shown in Fig. 4. The maximum value of NFDI corresponds to the damage location, and it can be seen from the figure that the recognition result is good.

Table 1

The measured frequencies and normalized RNFC values

Damage situation	Natural frequency, Hz							
	1st	2nd	4th	5th	6th	9th	10th	11th
No damage	2.45	15.36	43.01	84.29	139.37	208.25	290.97	387.56
100, mm	2.39	15.23	42.94	84.31	139.13	207.15	288.46	383.67
	1.00	0.37	0.08	0.00	0.08	0.23	0.37	0.43
700, mm	2.45	15.23	42.32	83.85	139.15	205.84	288.59	381.27
	0.00	0.55	0.98	0.35	0.14	0.73	0.53	1.00

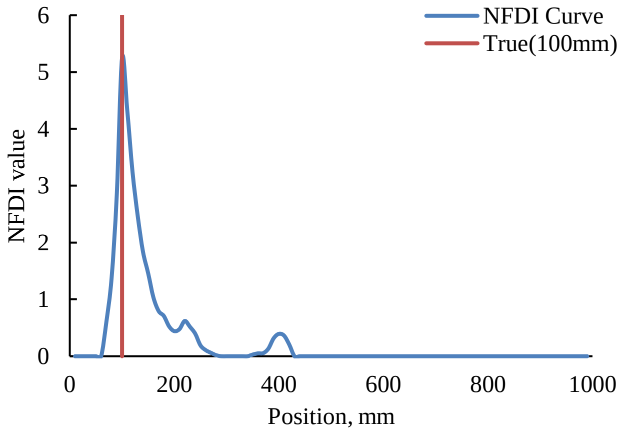

a

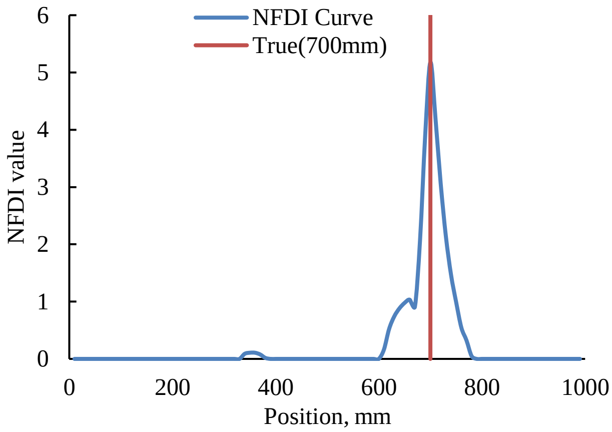

b

Fig. 4 The NFDI results under two damage conditions

3.2. Test for NFDI identification

The steel beam model was selected for test verification, and its size and material properties were the same as above. One end of the beam is fixed at 100 mm, and a 900 mm model is selected for analysis. The schematic diagram of the model and the actual structure are shown in Fig. 5, where the circle represents the position of the sensor. Acceleration sensors are used to obtain dynamic data, and the sensor information is shown in Table 2.

a

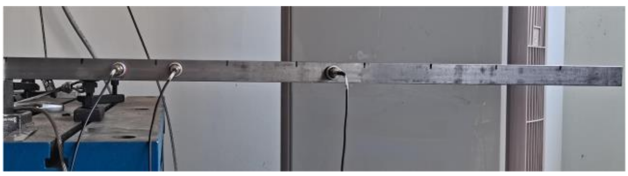

b

Fig. 5 The schematic diagram and structure of the model

Firstly, the normalized RNFC curve was calculated by modal analysis. As in Section 3.1, the boundary conditions of the model are cantilever beams. The sensors are placed on the surface of the beam and treated as mass points during the simulation process. The simulated damage conditions were set with 15 mm deep and 4 mm wide cracks at 100 mm intervals. The model has 8 damaged locations.

Considering the direction and accuracy of the signal obtained by the sensors, the frequencies of the transverse mode shape below 500 Hz are selected. Therefore, the 1st, 2nd, 4th, 5th, 6th, 9th, 10th, and 11th natural frequencies are selected for analysis. Then, the natural frequencies of the undamaged and damaged beams are obtained through simulation, and the normalized RNFC curves are established according to Eqs. (1) and (2). The results are shown in Fig. 6.

Table 2

The acceleration sensor information

Number	Position, mm	Range, V	Sensitivity, mv/G	Weight, g
1	450.0	10	96.39	43.1
2	225.0	10	98.52	42.8
3	150.0	10	97.53	43.0

Then, the natural frequencies of undamaged and damaged beams are obtained by tests. According to the cutting method, cut actual cracks of 15 mm deep and 4 mm wide at 100 mm and 700 mm respectively. The damaged beam is shown in Fig. 7.

The test adopts a dynamic signal analysis instrument. The analysis spectral line is 12800, the sampling points are 32768, the analysis frequency width is 500 Hz, the sampling frequency is 1280 Hz, and the sampling time of each frame is 25.6 s. The force hammer is used to stimulate the unit load, and the spectrum function obtained is shown in Fig. 8. The horizontal axis corresponding to the peak value is the natural frequency. To reduce the error, the measured frequency is obtained by three identical tests in each condition, and then the average value is taken as the measurement data. The measured results of various conditions are shown in Table 3. The measured RNFC values after normalization of all orders are calculated according to Eq. (5), and the results are also listed in Table 3.

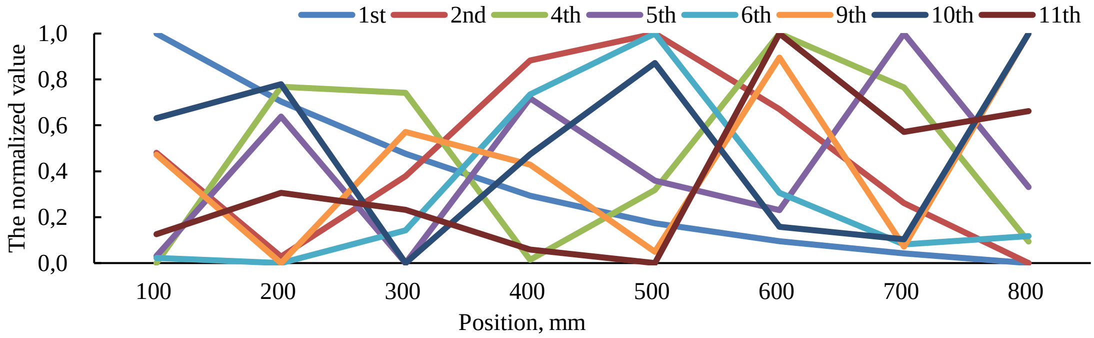

Fig. 6 The normalized curves of RNFC

Table 3

The measured frequencies and normalized RNFC values under the test

Damage situation	Natural frequency, Hz							
	1st	2nd	4th	5th	6th	9th	10th	11th
No damage	2.93	17.07	47.23	88.32	156.17	228.48	336.25	434.88
100, mm	2.89	17.11	47.42	88.24	155.63	226.76	333.98	433.36
	1.00	0.11	0.00	0.29	0.43	0.67	0.62	0.44
700, mm	3.01	17.25	46.88	86.62	156.50	227.42	335.47	429.34
	0.00	0.35	0.74	1.00	0.53	0.68	0.63	0.86

Fig. 7 The crack in the actual structure

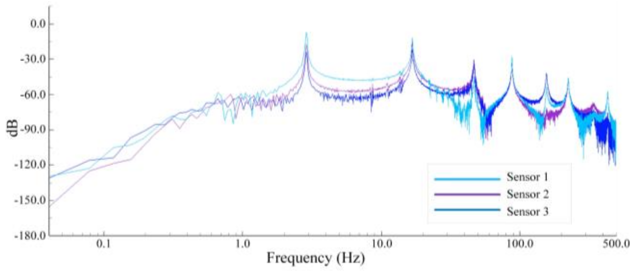

Fig. 8 The spectrum functions

Finally, the NFDI values are calculated according to Eqs. (6) to (13), and the results are shown in Fig. 9. The location of the maximum value in the figure is the identified damage location. The first condition identification effect is accurate, identifying the damage at the 100 mm position. In the second condition, there is an interference value, but the damage at 700 mm is still identifiable. Because the 700 mm position is close to the free end, the sensitivity is not large enough after damage. In other words, damage near the free end of the structure has less effect on the overall structure, resulting in less natural frequency variation and more susceptible to interference. In addition, the interference value may be generated due to insufficient frequency orders or noise in the test. In practice, all singular locations can be further detected as potential damages to avoid omissions.

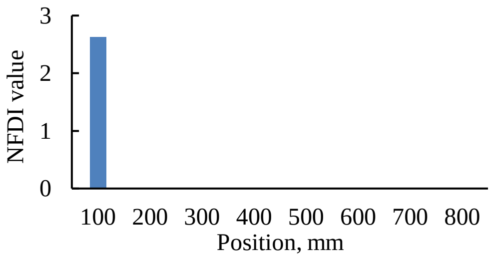

a) True (100 mm)

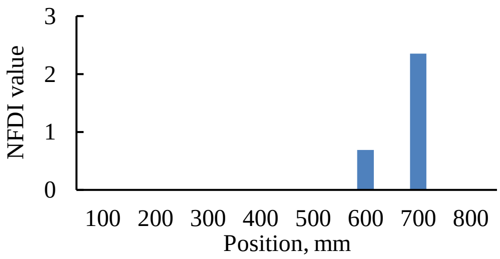

b) True (700 mm)

Fig. 9 The NFDI results of damage positions at 100 mm and 700 mm

3.3. The model updating with or without NFDI identification

After the damage location is identified by the Bayesian theory, the parameters of the location can be employed to identify the damage degree. This section compares the effects of model updating with or without NFDI identification. The model is updated using the Integrated Software Platform of Engineering and Scientific Computing (SiPESC), which loads and invokes plug-ins to complete the calculation process. The beam model in section 3.2 is imported into SiPESC for format standardization. The model is divided into 9 parts, with one parameter set for each part, as shown in Fig. 10. The damage condition is set as the elastic modulus of the 1st part is reduced from 2.0×10^{11} Pa to 1.8×10^{11} Pa, and the elastic modulus of the 2nd to 9th part is maintained at 2.0×10^{11} Pa. With structural strain data as residuals, the SQP optimization algorithm is used to update the model. The console outputs the iterative process and the optimal solution.

Fig. 10 The partitioned beam model

In the absence of NFDI identification, all 9 parameters should be selected for model updating. The results are shown in Fig. 11. It can be seen that the effect is not ideal and there is local convergence.

The NFDI values are calculated based on Bayesian theory to determine the damage location, and only the parameters at the damage location (assuming the 1st part is identified) should be selected for model updating. The result is shown in Fig. 12. It can be seen that the correction result is accurate and the iteration is rapid.

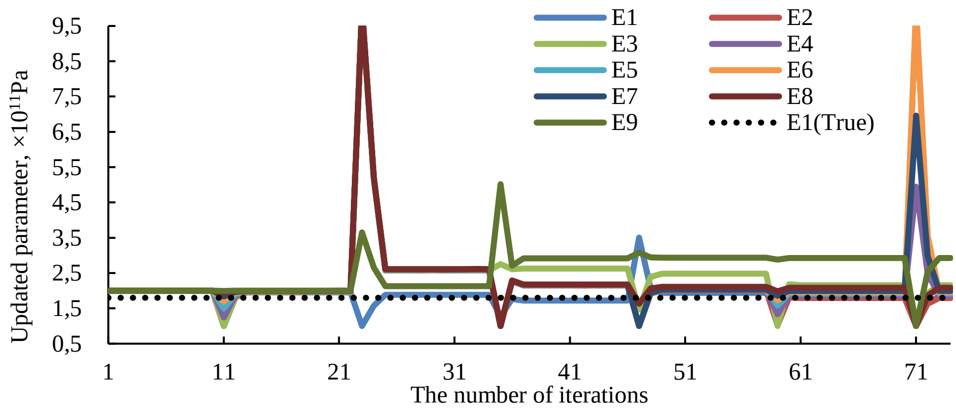

Fig. 11 The iteration results without NFDI identification

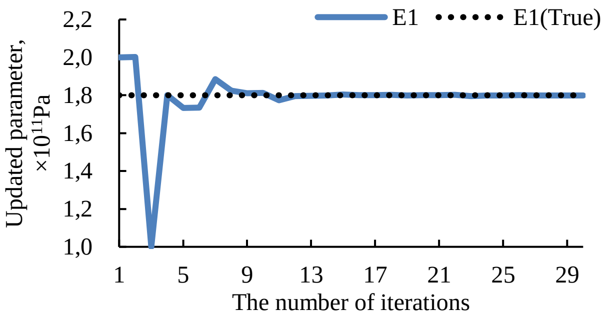

Fig. 12 The iteration result with NFDI identification

4. Verification of pressure container for the improved objective function

In this section, a pressure container is taken as an example to verified that the improved objective function will produce more accurate updated results. The sensitivity analysis of the model is performed, and the sensitivity coefficient is calculated to determine the weight. Then the updating effect of the SAC and OLS type objective function is compared.

The FE model of the pressure container is shown in Fig. 13 and the material parameters are shown in Table 4. The model consists of shell elements and beam elements, with a total of 202,051 elements, 185,452 nodes, and 1101,842 degrees of freedom. The load is the outward pressure exerted on the inside of the container. All degrees of freedom at the bottom of the container are restricted.

Table 4

The material parameters

Portion	Elastic modulus, $\times10^{11}$Pa	Poisson ratio	Density, kg/m^3
Base	2.09	0.3	7850
Inside	2.00	0.3	7850
Shell	2.09	0.3	7850

Fig. 13 The FE model of the pressure container

Firstly, the sensitivity coefficients are calculated and the weights are obtained. This section only updates the model of the shell portion. The updated shell is divided into 5 parts. Each part is divided into 9 sub-parts, and the sensitivity value of each sub-part is calculated. Then the sensitivity coefficients are calculated according to Eqs. (17) to (19). The fitting coefficients are shown in Table 5, and the fitting curves are shown in Fig. 14. It can be concluded that the front sensitivity coefficient is the largest. Then the weights of the objective function are calculated according to Eqs. (1) and (2), which are also given in Table 5.

Table 5

The fitting coefficient of each part

ID	Coefficient b	Coefficient μ	Correlation index	Weight w
1 (Left)	0.428	4.546	0.962	0.129
2 (Right)	0.432	2.840	0.973	0.130
3 (Front)	1.363	0.458	0.997	0.410
4 (Back)	0.670	0.287	1.000	0.201
5 (Top)	0.434	2.734	0.962	0.130

Then the effect of the improved objective function is verified, and the objective functions of the SAC type and the OLS type are compared. The elastic modulus for part 1-

5 is used as the updated parameters. The SQP algorithm is also used to update the model. The updated parameters and results of the model are shown in Table 6, and the absolute values of errors are shown in Fig. 15. The results show that the errors of the OLS type objective function are within 5%, while the errors of the SAC type are within 2%. The model updating result of the SAC type is better, which verifies the updated accuracy of the improved objective function.

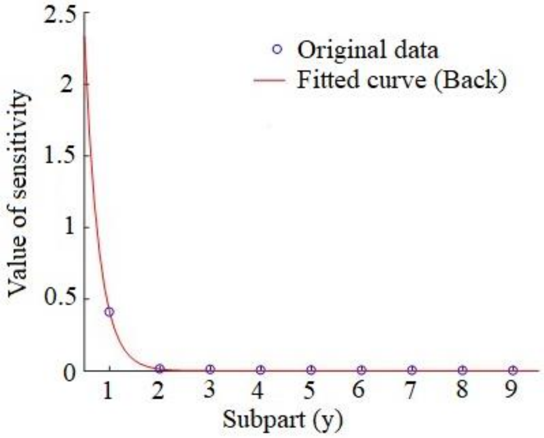

Fig. 14 The fitting curves of one part

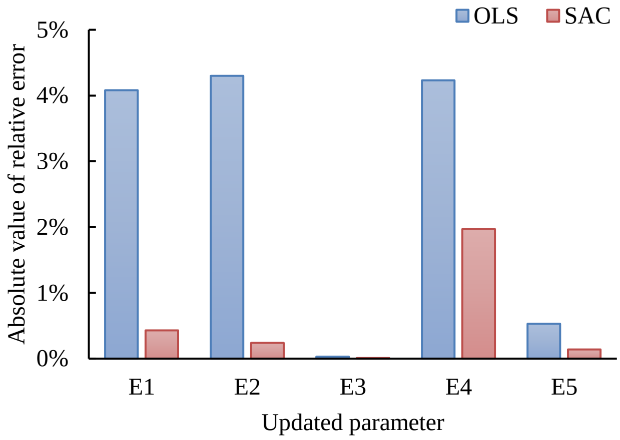

Fig. 15 The result errors of different objective functions

Table 6

The updated parameters and results of model updating

Method	Updated parameters	Initial value, $\times 10^{11}$Pa	Updated value, $\times 10^{11}$Pa	Actual value, $\times 10^{11}$Pa	Error, %
OLS	E1	2.00000	2.00463	2.09000	-4.08
	E2	2.00000	2.00008	2.09000	-4.30
	E3	2.00000	2.09072	2.09000	0.03
	E4	2.00000	2.00169	2.09000	-4.23
	E5	2.00000	2.07886	2.09000	-0.53
SAC	E1	2.00000	2.08112	2.09000	-0.43
	E2	2.00000	2.08494	2.09000	-0.24
	E3	2.00000	2.09011	2.09000	0.01
	E4	2.00000	2.04881	2.09000	-1.97
	E5	2.00000	2.08702	2.09000	-0.14

5. Conclusions

The methods to improve the efficiency and accuracy of FE model updating have been proposed in this paper. The selection of updated parameters has been improved based on the Bayesian theory, and a more reasonable objective function is proposed based on the strain assurance criterion with weight terms determined according to the sensitivity coefficient. Through numerical examples and test verification, the following conclusions can be drawn:

1. The NFDI based on Bayesian theory can accurately identify the damage location.

2. The proposed model updating method combined with Bayesian theory can improve the selection of updated parameters.

3. The proposed sensitivity coefficient can quantify the sensitivity of the model and be used to set the weights in the objective function.

4. For the objective function of model updating, the proposed SAC type is more accurate than the OLS type.

Declaration of Conflicting Interests

The authors declare no conflict of interest in preparing this article.

Data Availability Statement

No data were used to support this study.

References

1. **Garcia-Palencia, A. J.; Santini-Bell, E.; Sipple, J. D.; Sanayei, M.** 2015. Structural model updating of an in-service bridge using dynamic data, Structural Control and Health Monitoring 22(10): 1265-1281. http://dx.doi.org/10.1002/stc.1742.
2. **Zhan, J.; Wang, C.; Yan, Y.; Deng, L.; Zhu, W.; Liu, J.** 2022. Modal analysis and condition evaluation of substructures for simply supported high-speed railway bridge based on a simplified model, Journal of Bridge Engineering 27(8): 04022058. http://dx.doi.org/10.1061/(ASCE)BE.1943-5592.0001900.
3. **Weng, S.; Zhu, H.; Xia, Y.; Li, J.; Tian, W.** 2020. A review on dynamic substructuring methods for model updating and damage detection of large-scale structures, Advances in Structural Engineering 23(3): 584-600. http://dx.doi.org/10.1177/1369433219872429.
4. **Bartilson, D. T.; Jang, J.; Smyth, A. W.** 2020. Sensitivity-based singular value decomposition parametrization and optimal regularization in finite element model updating, Structural Control and Health Monitoring 27(6): e2539. http://dx.doi.org/10.1002/stc.2539.
5. **Chhipa, S. M.; Kumar, P.; Bagha, A. K.; Bahl, S.** 2021. Removing uncertainty in the boundary condition of five degree of freedom spring mass vibratory system

using direct updating method, Materials Today: Proceedings 41: 251-255. http://dx.doi.org/10.1016/j.matpr.2020.08.803.

6. **Yuan, Z.; Liang, P.; Silva, Y.; Yu, K.; Mottershead, J. E.** 2019. Parameter selection for model updating with global sensitivity analysis, Mechanical Systems and Signal Processing 115: 483-496. http://dx.doi.org/10.1016/j.ymssp.2018.05.048.
7. **Zhang, Y.; Zhao, Y.; Ouyang, H.** 2022. Stochastic model updating for assembled structures with bolted joints using a Bayesian method, Engineering Optimization 54(11): 1919-1937. http://dx.doi.org/10.1080/0305215X.2021.1965136.
8. **Nityananda, R. H.; Srivatsa, S. R.; Somaskanda, S.; Pasha, T. A.** 2021. Finite element model updating of boring bar and determination of chatter stability, Materials Today: Proceedings 45: 165-171. http://dx.doi.org/10.1016/J.MATPR.2020.10.411.
9. **Pan, Y.; Ventura, C. E.; Xiong, H.; Zhang, F. L.** 2020. Model updating and seismic response of a super tall building in Shanghai, Computers and Structures 239: 106285. http://dx.doi.org/10.1016/j.compstruc.2020.106285.
10. **Zhu, T.; Zhang, G.; Zang, C.** 2022. Frequency-domain nonlinear model updating based on analytical sensitivity and the Multi-Harmonic balance method, Mechanical Systems and Signal Processing 163: 108169. http://dx.doi.org/10.1016/J.YMSSP.2021.108169.
11. **Ouyang, H.; Liu, J.; Li, Z.; Han, X.** 2022. A novel dynamic model updating method for composite laminate structures considering non-probabilistic uncertainties and correlations, Composite Structures 287: 115359. http://dx.doi.org/10.1016/J.COMPSTRUCT.2022.115359.
12. **Pan, Q. J.; Zhang, R. F.; Ye, X. Y.; Li, Z. W.** 2021. An efficient method combining polynomial-chaos kriging and adaptive radial-based importance sampling for reliability analysis, Computers and Geotechnics 140: 104434. http://dx.doi.org/10.1016/J.COMPGEO.2021.104434.
13. **Li, X. Q.; Song, L. K.; Bai, G. C.** 2022. Vectorial surrogate modeling approach for multi-failure correlated probabilistic evaluation of turbine rotor, Engineering with Computers: 1-20. http://dx.doi.org/10.1007/S00366-021-01594-2.
14. **Xiang, Y.; Pan, B.; Luo, L.** 2021. A new model updating strategy with physics-based and data-driven models, Structural and Multidisciplinary Optimization 64: 163-176. http://dx.doi.org/10.1007/S00158-021-02868-5.
15. **Lin, S. W.; Du, Y. L.; Yi, T. H.; Yang, D. H.** 2022. Model updating using bridge influence lines based on an adaptive metamodel global optimization method, Journal of Bridge Engineering 27(3): 04022003. http://dx.doi.org/10.1061/(ASCE)BE.1943-5592.0001839.
16. **Şahin, A.; Bayraktar, A.** 2014. Computational finite element model updating tool for modal testing of structures, Structural Engineering and Mechanics 51(2): 229-248. http://dx.doi.org/10.12989/SEM.2014.51.2.229.
17. **Qin, S.; Hu, J.; Zhou, Y.; Zhang, Y.; Kang, J.** 2019. Feasibility study of improved particle swarm optimization in kriging metamodel based structural model updating, Structural Engineering and Mechanics 70(5): 513-524. http://dx.doi.org/10.12989/sem.2019.70.5.513.
18. **Caicedo, J. M.; Yun, G. J.** 2011. A novel evolutionary algorithm for identifying multiple alternative solutions in model updating, Structural Health Monitoring 10(5): 491-501. http://dx.doi.org/10.1177/1475921710381775.
19. **Li, D.; Zhang, J.** 2023. Finite element model updating through derivative-free optimization algorithm, Mechanical Systems and Signal Processing 185: 109726. http://dx.doi.org/10.1016/J.YMSSP.2022.109726.
20. **Bagha, A. K.; Tiwari, S.; Kumari, S.; Samyal, R.; Bedi, R.; Sharma, N.; Bahl, S.** 2022. Finite element model updating of microwave welded lap joint with direct updating algorithm, Physica Scripta 97(8): 085704. http://dx.doi.org/10.1088/1402-4896/AC7EFD.
21. **Qin, S.; Yuan, Y.; Gan, Y.; Wang, Q.** 2022. Improved metaheuristic algorithm based finite element model updating of a hybrid girder cable-stayed railway bridge, Buildings 12(7): 958. http://dx.doi.org/10.3390/BUILDINGS12070958.
22. **Xu, G.; Azhari, F.** 2021. Predicting the remaining useful life of corroding bridge girders using Bayesian updating, Journal of Performance of Constructed Facilities 35(5): 04021055. http://dx.doi.org/10.1061/(ASCE)CF.1943-5509.0001626.
23. **Barman, S. K.; Mishra, M.; Maiti, D. K.; Maity, D.** 2021. Vibration-based damage detection of structures employing Bayesian data fusion coupled with TLBO optimization algorithm, Structural and Multidisciplinary Optimization 64: 2243-2266. http://dx.doi.org/10.1007/S00158-021-02980-6.
24. **Ierimonti, L.; Cavalagli, N.; Venanzi, I.; García-Macías, E.; Ubertini, F.** 2021. A transfer Bayesian learning methodology for structural health monitoring of monumental structures, Engineering Structures 247: 113089. http://dx.doi.org/10.1016/J.ENGSTRUCT.2021.113089
25. **Lam, H. F.; Hu, J.; Zhang, F. L.; Ni, Y. C.** 2019. Markov chain Monte Carlo-based Bayesian model updating of a sailboat-shaped building using a parallel technique, Engineering Structures 193: 12-27. http://dx.doi.org/10.1016/j.engstruct.2019.05.023.
26. **Yuan, Z.; Liang, P.; Silva, T.; Yu, K.; Mottershead, J. E.** 2019. Parameter selection for model updating with global sensitivity analysis, Mechanical Systems and Signal Processing 115: 483-496. http://dx.doi.org/10.1016/j.ymssp.2018.05.048.
27. **Sha, G.; Radzieński, M.; Cao, M.; Ostachowicz, W.** 2019. A novel method for single and multiple damage detection in beams using relative natural frequency changes, Mechanical Systems and Signal Processing 132: 335-352. http://dx.doi.org/10.1016/j.ymssp.2019.06.027.
28. **Zhu, Y. H.; Zhao, Y. F.; Wang, J. X.** 2017. Research on information fusion optimization algorithm of ceramic shuttle kiln temperature based on multi-sensor, Journal of Computational Methods in Sciences and Engineering 17(4): 655-664. http://dx.doi.org/10.3233/JCM-170749.

M. Zhai, Y. Xie

MODEL UPDATING BASED ON BAYESIAN THEORY AND IMPROVED OBJECTIVE FUNCTION

S u m m a r y

Model updating is the process of calibrating model parameters to improve the accuracy of numerical prediction. To improve the accuracy and efficiency of model updating, this paper proposes a model updating method based on Bayesian theory and improved objective function. A natural frequency damage index is proposed based on the Bayesian theory, which is calculated according to the established damage position function and the measured frequency data. The distribution of the index can determine the damage location and the number of updated parameters for model updating. An objective function with weight terms is proposed based on strain assurance criterion to describes the difference between the finite element model and the actual structure, and the weight term of the objective function is determined by the sensitivity coefficient. Examples show that the improved model updating method is more accurate and efficient.

Keywords: model updating, Bayesian theory, sensitivity coefficient, strain assurance criterion.

Received January 20, 2023
Accepted October 9, 2023